Pergamon

SCIENCE DIRECT®

Bioorganic & Medicinal Chemistry Letters 13 (2003) 83–86

BIOORGANIC & MEDICINAL CHEMISTRY LETTERS

Fluorescent Bioprobes for Visualization of Puromycin-Sensitive Aminopeptidase in Living Cells

Hiroki Kakuta, Yukiko Koiso, Kazuo Nagasawa and Yuichi Hashimoto*

Institute of Molecular and Cellular Biosciences, The University of Tokyo, 1-1-1 Yayoi, Bunkyo-ku, Tokyo 113-0032, Japan

Received 30 August 2002; accepted 1 October 2002

Abstract—Non-peptide, small-molecular, non-competitive inhibitors of puromycin-sensitive aminopeptidase (PSA), that is, 3-(2,6-diethylphenyl)-2,4(1*H*,3*H*)-quinazolinedione (PAQ-22, **3**) and its 1*N*-methyl analogue (MPAQ-22 **4**), were structurally modified to afford fluorescent bioprobes, ANTAQ (**5**) and DAMPAQ-22 (**6**). The cellular localization of PSA could be visualized by the use of these fluorescent bioprobes.

Puromycin-sensitive aminopeptidase (PSA: EC 3.4.11.14), which is a neutral aminopeptidase with a substrate specificity similar to that of aminopeptidase N (APN), is distributed mainly in the brain and neurons.[1–7] Though this enzyme was first isolated as a candidate for enkephalinase,[1–3,5] and it has been reported that PSA gene-deficient mice obtained by a mouse gene-trapping method show increased anxiety and impaired pain response,[8] the physiological role(s)/function(s) of PSA remain unclear because of the low substrate specificity of the enzyme and the lack of specific inhibitors.[5–8] The localization of PSA at the cell structural level is still not known.

Recently, we have reported potent non-peptide, small-molecular PSA-specific inhibitors with a homophthalimide or a quinazolinedione skeleton derived from thalidomide (**1**), including *N*-(2,6-diethylphenyl)homophthalimide (PIQ-22, **2**), 3-(2,6-diethylphenyl)-2,4(1*H*,3*H*)-quinazolinedione (PAQ-22, **3**) and 1-methyl-3-(2,6-diethylphenyl)-2,4(1*H*,3*H*)-quinazolinedione (MPAQ-22, **4**) (Fig. 1).[9–16] They are all potent PSA-specific non-competitive inhibitors with IC_{50} values of 3–8 μM (Table 1). The potencies of these inhibitors are comparable to those of bestatin and actinonin (competitive inhibitors).[9–16] By employing these PSA inhibitors, we identified possible roles of the enzyme in cell mobility/invasion/apoptosis.[11–13,16,17]

For the investigation of the molecular/cell-level mechanism(s) of these PSA inhibitors and the physiological role(s) of PSA, preparation of PSA-specific bioprobes which are applicable to living cells is required. Here, we report the preparation of fluorescent bioprobes specific to PSA and their application to the visualization of PSA in living cells.

We chose PAQ-22 (**3**) and MPAQ-22 (**4**) as pharmacophores because of their superior chemical stability and bioavailability compared to those of PIQ-22 (**2**).[12,16]

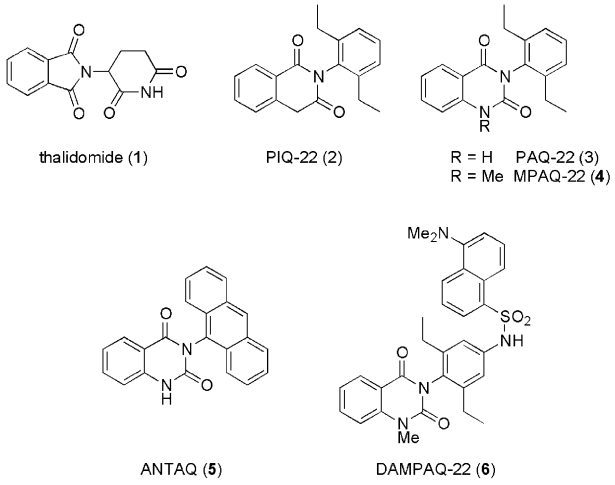

Figure 1. Structures of thalidomide (**1**), PSA-specific inhibitors (PIQ-22: **2**, PAQ-22: **3**, MPAQ-22: (**4**) derived from thalidomide, and the designed fluorescent bioprobes (ANTAQ: **5**, DAMPAQ-22: **6**).

*Corresponding author. Tel.: +81-3-5841-7847; fax: +81-3-5841-8495; e-mail: hashimot@iam.u-tokyo.ac.jp

0960-894X/03/$ - see front matter © 2002 Elsevier Science Ltd. All rights reserved.
PII: S0960-894X(02)00845-4

For derivatization of PAQ-22 (**3**)/MPAQ-22 (**4**) to fluorescent analogues, two strategies were applied on the basis of the results of our previous structure–activity relationship studies,[9–16] that is (i) derivatization of the 2,6-diethylphenyl group, which is critical for potent PSA-inhibiting activity, to a fluorescent 9-anthracenyl group, and (ii) introduction of a fluorescent dansyl group into the 2,6-diethylphenyl group at the 4-position, which was not expected to drastically affect the activity. Thus, we designed ANTAQ (**5**) and DAMPAQ-22 (**6**) (Fig. 1).

ANTAQ (**5**) was prepared by condensation of 9-aminoanthracene and methyl anthranilate in the presence of triphosgene by the method described previously (Fig. 2).[15] DAMPAQ-22 (**6**) was prepared by condensation of dansyl chloride and 1-methyl-3-(2,6-diethyl-4-aminophenyl)-2,4(1*H*,3*H*)-quinazolinedione, which was itself prepared by condensation of 2,6-diethyl-4-nitroaniline with methyl anthranilate in the presence of triphosgene followed by reduction of the nitro group to an amino group (Fig. 2). The structures of the prepared compounds were confirmed by ^{1}H NMR, mass spectroscopy, and elemental analysis, which gave appropriate analytical values.[18,19]

As expected, ANTAQ (**5**) and DAMPAQ-22 (**6**) showed potent PSA-inhibiting activity and possessed high fluorescence intensity.[18,19] Their PSA-inhibiting activity was comparable to those of the mother compounds, PAQ-22 (**3**) and MPAQ-22 (**4**), with IC_{50} values of 2.9 and 4.6 μM, respectively (Table 1). They are inactive toward APN and dipeptidylpeptidase type IV, as are PAQ-22 (**3**), MPAQ-22 (**4**) and PIQ-22 (**2**), indicating that they are specific to PSA. Lineweaver–Burk plot analysis (Fig. 3) indicated that ANTAQ (**5**) and DAMPAQ-22 (**6**) act as non-competitive inhibitors, as do PAQ-22 (**3**), MPAQ-22 (**4**) and PIQ-22 (**2**).[11–16] In addition, they are easily incorporated into living human monocytic cells MOLT-4 under the general cell culture conditions (vide infra), and showed no apparent cytotoxicity within the concentration range used in the experiments, as far as could be judged by optical and fluorescence microscopy.

Table 1. PSA-inhibitory activity of compounds **2**–**6**

Compd	Inhibition IC_{50}, μM[a]	Compd	Inhibition IC_{50}, μM[a]
PIQ-22: **2**	7.8	ANTAQ: **5**	2.9
PAQ-22: **3**	3.8	DAMPAQ-22: **6**	4.6
MPAQ-22: **4**	3.4		

[a]PSA-inhibitory activity was assayed by the use of L-Ala-AMC with MOLT-4.[9–16]

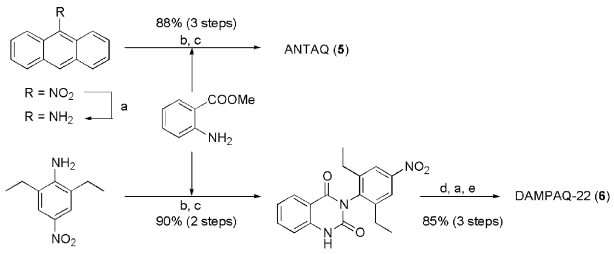

Figure 2. Synthesis of ANTAQ (**5**) and DAMPAQ-22 (**6**).

We first checked the applicability of ANTAQ (**5**) and DAMPAQ-22 (**6**) as fluorescent bioprobes to visualize PSA in living cells by the use of four types of cells, that

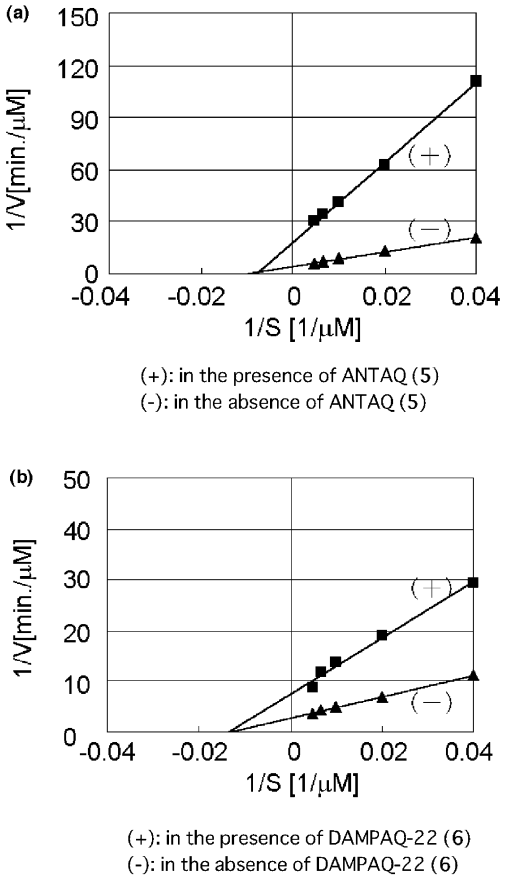

Figure 3. Lineweaver–Burk plot analysis of PSA inhibition by (a) ANTAQ (**5**) and (b) DAMPAQ-22 (**6**).

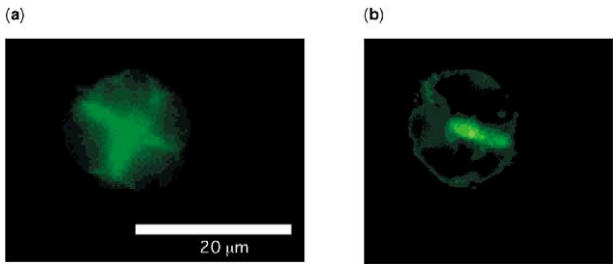

Figure 4. Fluorescent microscopic images of MOLT-4 cells treated with 10 μM (a) ANTAQ (**5**) or (b) DAMPAQ-22 (**6**) for 10 min at 37 °C. U-MNUA2 filter (Ex/Em: 360/405 nm) and U-WU2 filter (Ex/Em: 360/510 nm) were used for panels (a) and (b), respectively.

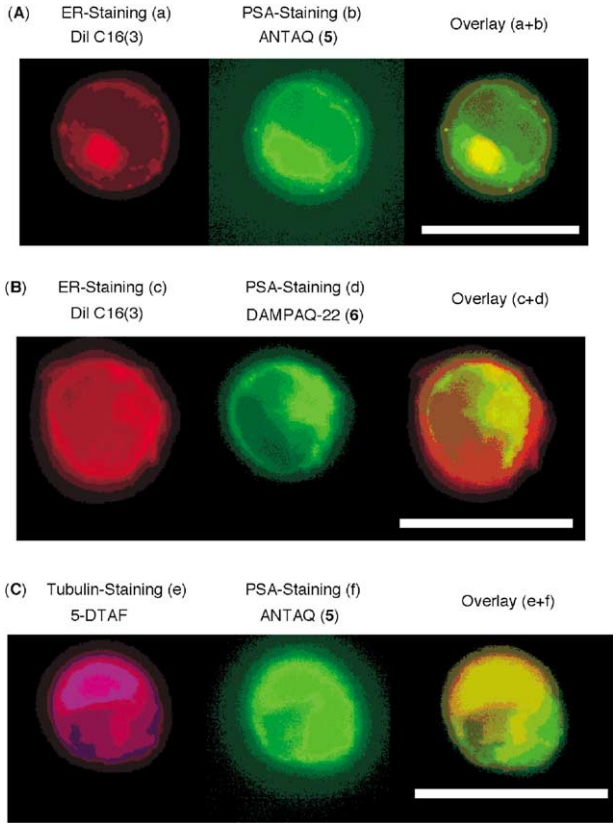

Figure 5. Fluorescence microscopic images of MOLT-4 cells treated with ANTAQ (**5**), DAMPAQ (**6**), Dil C16(3) and 5-DTAF. (A) Dil C16(3) (1 μM, ER staining), ANTAQ (**5**, 10 μM, PSA staining), for 10 min at 37 °C, and their overlay. (B) Dil C16(3) (1 μM, ER staining), DAMPAQ-22 (**6**, 10 μM, PSA staining), for 10 min at 37 °C, and their overlay. (C) 5-DTAF (1 μM, tubulin staining), ANTAQ (**5**, 10 μM, PSA staining). White bars in the overlay panels indicate 20 μm. Filters used for ANTAQ (**5**) and DAMPAQ-22 (**6**) were the same as Figure 4. For Dil C16(3) and 5-DTAF, U-WIG2 filter (Ex/Em: 549/565 nm) was used.

is, human monocytic cell line MOLT-4, which is known to express PSA,[9–16] human leukemia cell line HL-60, which lacks or only weakly expresses PSA,[12,16] and COS-1 cells transfected or not transfected with a PSA expression vector. As expected, MOLT-4 and PSA-transfected COS-1 cells (cells expressing PSA) were efficiently stained by ANTAQ (**5**) or DAMPAQ-22 (**6**), while HL-60 and non-treated COS-1 cells (cells lacking or weakly expressing PSA) were not stained or were only weakly stained (no localized staining was observed). The ratio of the fluorescence intensity of MOLT-4 and HL-60 stained by DMAPAQ-22 (**6**) was 11:3. The results indicated that both ANTAQ (**5**) and DAMPAQ-22 (**6**) are superior fluorescent bioprobes for visualization of PSA in living cells. The fluorescent microscopic observation of MOLT-4 cells treated with ANTAQ (**5**) and DAMPAQ-22 (**6**) suggested a specific localization pattern of PSA in the cells. Typical images are shown in Figure 4, though the localization pattern is not entirely uniform among the cells.

Comparison of the photographs of fluorescence images (Fig. 4) with optical microscopic images (not shown) of MOLT-4 cells with or without Wright–Giemsa staining suggested that PSA exists in the cytosolic fraction, not in the nucleus, which is in accordance with our previous results.[9–16] Moreover, PSA seemed to be localized at the cleft or groove of karyolobism (lobulated nucleus) in the cell.

In order to gain further information concerning the distribution/localization of PSA in living cells, fluorescent staining with other probes, including Dil C16(3) [which has been established to stain endoplasmic reticulum (ER), Molecular Probes Co. Ltd.] and 5-DTAF (which has been established to stain tubulin, Molecular Probes Co. Ltd.), was carried out (Fig. 5).

In the overlaid images in Figure 5 (the right images in panels A–C), areas colored with yellow/orange indicate co-localization of PSA (colored green in the middle images in panels A–C) with ER (colored with red in the left images in panels A and B) or tubulin (colored with purple in the left image in the panel C). At first glance, PSA seems to co-localize with both ER and tubulin. However, the yellow areas in the overlaid images in panels A and B are much smaller than that observed in the overlaid image in panel C. The results suggest that PSA is distributed in a manner which is more similar to tubulin than to ER. Further investigation of the effects of PSA inhibitors on cell mobility/invasion and apoptosis is scheduled.

In conclusion, PSA-specific fluorescent bioprobes, ANTAQ (**5**) and DAMPAQ-22 (**6**), were prepared by structural modification of our potent PSA-specific inhibitors. The usefulness of these bioprobes for visualization of PSA in living cells was demonstrated. Because these bioprobes also possess potent PSA-inhibiting activity, they should be useful tools to investigate so far unknown physiological role(s) of PSA.

Acknowledgements

The work described in this paper was partially supported by Grants-in-Aid from the Ministry of Education, Culture, Sports, Science and Technology of Japan. The authors are grateful to Dr. Akimitsu, Mr. Miyagi, and Mr. Ogawa (Olympus Co. Ltd.) for their technical support in obtaining fluorescence microscopic photographs.

References and Notes

1. Hersh, L. B.; McKelvy, J. F. *J. Neurochem.* **1981**, *36*, 171.
2. McLellan, S.; Dyer, S. H.; Hersh, L. B. *J. Neurochem.* **1988**, *51*, 1552.
3. Johnson, G. D.; Hersh, L. B. *Arch. Biochem. Biophys.* **1990**, *276*, 305.
4. Rawlings, N. D.; Barrett, A. J. *Biochem. J.* **1993**, *290*, 201.
5. Tobler, A. R.; Constam, D. B.; Schmitt-Graff, A.; Malipiero, U.; Schlabach, R.; Fontana, A. *J. Neurochem.* **1997**, *68*, 889.
6. Costam, D. B.; Tobler, A. R.; Rensing-Ehl, A.; Kelmer, I.; Hersh, L. B.; Fontana, A. *J. Biol. Chem.* **1995**, *270*, 26931.
7. Bauer, M. O.; Nanda, I.; Beck, G.; Schmid, M.; Jacob, F. *Cytogenet. Cell Genet.* **2001**, *92*, 221.
8. Osada, T.; Ikegami, S.; Takiguchi-Hayashi, K.; Yamazaki, Y.; Katoh-Fukui, Y.; Higashikanagawa, T.; Sasaki, Y.; Takeuchi, T. *J. Neurochem.* **1999**, *19*, 6068.
9. Hashimoto, Y. *Bioorg. Med. Chem.* **2002**, *10*, 461.
10. Hashimoto, Y. *Curr. Med. Chem.* **1998**, *5*, 163.
11. Shimazawa, R.; Takayama, H.; Fujimoto, Y.; Komoda, M.; Dodo, K.; Yamasaki, Y.; Shirai, R.; Koiso, Y.; Miyata, K.; Kato, F.; Kato, M.; Miyachi; Hashimoto, Y. *J. Enzyme Inhibit.* **1999**, *14*, 259.
12. Takahashi, H.; Komoda, M.; Kakuta, H.; Hashimoto, Y. *Yakugaku Zasshi* **2000**, *120*, 909.
13. Kakuta, H.; Takahashi, H.; Sou, S.; Kita, T.; Nagasawa, K.; Hashimoto, Y. *Recent Res. Develop. Med. Chem.* **2001**, *1*, 189.
14. Miyachi, H.; Kato, M.; Kato, F.; Hashimoto, Y. *J. Med. Chem.* **1998**, *41*, 263.
15. Kakuta, H.; Koiso, Y.; Takahashi, H.; Nagasawa, K.; Hashimoto, Y. *Heterocycles* **2001**, *55*, 1433.
16. Komoda, M.; Kakuta, H.; Takahashi, H.; Fujimoto, Y.; Kadoya, S.; Kato, F.; Hashimoto, Y. *Bioorg. Med. Chem.* **2001**, *9*, 121.
17. Kagechika, H.; Komoda, M.; Fujimoto, Y.; Koiso, Y.; Takayama, H.; Kadoya, S.; Miyata, K.; Kato, F.; Kato, M.; Hashimoto, Y. *Biol. Pharm. Bull.* **1999**, *22*, 1010.
18. 3-(9-Anthracenyl)-2,4(*1H,3H*)-quinazolinedione (ANTAQ: **5**) Pale yellow cubes from EtOAc; mp >300 °C; ^{1}H NMR (500 MHz, DMSO-d_6) δ: 16.60 (s, 1H), 8.78 (s, 1H), 8.20 (d, 2H, $J=7.5$ Hz), 7.98 (d, 1H, $J=7.5$ Hz), 7.82 (d, 2H, $J=7.5$ Hz), 7.80 (t, 1H, $J=7.5$ Hz), 7.57 (t, 2H, $J=7.5$ Hz), 7.51 (t, 2H, $J=7.5$ Hz), 7.38 (d, 1H, $J=7.5$ Hz), 7.30 (t, 1H, $J=7.5$ Hz); FAB-MS m/z: 339 $(M+H)^+$. Anal. calcd for $C_{22}H_{14}N_2O_2$ C, 78.09; H, 4.17; N, 8.28. Found: CHN. Wavelengths of the maximum fluorescence intensity (Ex/Em): 360/405 nm (benzene), 370/405 nm (CH_2Cl_2), 360/405 nm (MeOH).
19. 3-(2,6-Diethyl-4-dansylaminophenyl)-1-methyl-2,4(*1H,3H*)-quinazolinedione (DAMPAQ-22: **6**). Pale green cubes from MeOH; mp 244 °C; ^{1}H NMR (500 MHz, $CDCl_3$) δ: 8.50 (d, 1H, $J=8.0$ Hz), 8.39 (d, 1H, $J=8.0$ Hz), 8.25 (d, 1H, $J=8.0$ Hz), 8.24 (d, 1H, $J=8.0$ Hz), 7.74 (td, 1H, $J=8.0$, 1.5 Hz), 7.55 (t, 1H, $J=8.0$ Hz), 7.46 (d, 1H, $J=8.0$ Hz), 7.44 (s, 1H), 7.29 (t, 1H, $J=8.0$ Hz), 7.28 (t, 1H, $J=8.0$ Hz), 7.17 (d, 1H, $J=8.0$ Hz), 6.68 (s, 2H), 3.66 (s, 3H), 2.87 (s, 6H), 2.23 (q, 2H, $J=7.5$ Hz), 2.24 (q, 2H, $J=7.5$ Hz), 0.91 (t, 6H, $J=7.5$ Hz); FAB-MS m/z: 556 $(M)^+$, 557 $(M+H)^+$. Anal. calcd for $C_{31}H_{32}N_4O_4$: C, 66.88; H, 5.79; N, 10.06. Found: C, 66.72; H, 5.85; N, 10.04. Wavelengths of the maximum fluorescence intensity (Ex/Em): 320/490 nm (benzene), 320/510 nm (CH_2Cl_2), 320/510 nm (MeOH).
20. Shimazawa, R.; Hibino, S.; Mizoguchi, H.; Hashimoto, Y.; Iwasaki, S.; Kagechika, H.; Shudo, K. *Biochem. Biophys. Res. Comm.* **1991**, *180*, 249.
21. Hashimoto, Y.; Shimazawa, R. *Clin. Dermatol.* **1993**, *5*, 585.
22. Sawada, T.; Kato, Y.; Kobayashi, H.; Hashimoto, Y.; Watanabe, T.; Sugiyama, Y.; Iwasaki, S. *Bioconjugate Chem.* **1993**, *4*, 284.